The Canadian Mineralogist
Vol. 35, pp. 947-958 (1997)

TEXTURE AND STRUCTURE OF OPAL-CT AND OPAL-C IN VOLCANIC ROCKS

TOSHIRO NAGASE[1] AND MIZUHIKO AKIZUKI

Institute of Mineralogy, Petrology and Economic Geology, Faculty of Science, Tohoku University, Aoba, Sendai 980-77, Japan

ABSTRACT

Textures and structures of opal-CT and opal-C in volcanic rocks from the Hosaka and Akase opal mines in Japan were studied using an optical microscope and scanning and transmission electron microscopes. Textures of the opal-CT are optically classified into anisotropic columnar and isotropic massive (opal-CT_M) types. Both textures consist of thin and platy crystals showing two wide {101} faces of low cristobalite. Images obtained by high-resolution transmission electron microscopy show that the cristobalite structure is the fundamental component of volcanic-type opal-CT, and that many stacking faults are present randomly in the structure. Columns are produced by parallel growth of platy crystals; opal-CT_M and lepispheres consist of criss-crossing aggregates of blades. Each blade is composed of roughly parallel aggregates of platy crystals. The variation of d_{101} values with textural and structural changes of the opal-CT was measured by an X-ray powder-diffraction method. With decrease of d_{101} value, highly ordered cristobalite domains develop surrounding the domains of disordered cristobalite in the crystal. The considerable difference in degree of order of stacking between the two types of domain implies changes in the growth process of the crystal.

Keywords: opal-CT, opal-C, lepisphere, cristobalite, transmission electron microscopy, scanning electron microscopy, opal mines, Japan.

SOMMAIRE

Les textures et les structures de l'opale-CT et de l'opale-C dans les roches volcaniques des mines d'opale de Hosaka et d'Akase, au Japon, ont été étudiées par microscopies optique et électronique (en transmission et par balayage). Les textures de l'opale-CT sont classifiées optiquement en colonnes anisotropes et en masses isotropes (opale-CT_M). Dans les deux types de texture, il s'agit de minces cristaux en plaquette montrant deux faces {101} plus larges, typiques de la cristobalite ordonnée. Les images obtenues par microscopie électronique en transmission à haute résolution montrent que la structure de la cristobalite est l'élément fondamental de la structure de l'opale-CT de type volcanique, et que les défauts d'empilement se développent en grand nombre de façon aléatoire dans la structure. Les colonnes résultent de la croissance parallèle de cristaux en plaquette; opale-CT_M et lépisphères sont faits d'agrégats de lames enchevêtrées. Chaque lame est faite d'agrégats plus ou moins parallèles de cristaux en plaquette. La variation de d_{101} avec les aspects texturaux et structuraux de l'opale-CT a été mesurée par diffraction X sur poudre. A mesure que diminue la valeur de d_{101}, des domaines de cristobalite fortement ordonnée apparaissent autour des domaines de cristobalite désordonnée dans le cristal. La différence importante dans le degré d'ordre de l'empilement entre les deux sortes de domaines implique qu'il y a eu un changement de processus de croissance cristalline.

(Traduit par la Rédaction)

Mots-clés: opale-CT, opale-C, lépisphère, cristobalite, microscopie électronique par transmission, microscopie électronique par balayage, mines d'opale, Japon.

INTRODUCTION

Microcrystalline silica composed of stackings of both cristobalite and tridymite, as inferred from an X-ray-diffraction analysis (Jones & Segnit 1971, Graetsch *et al.* 1994), is referred to as "opal-CT". Opal-CT is often found in silicic sedimentary rocks and in nodules of silica within volcanic rocks. Segnit *et al.* (1970) were the first to report, on the basis of scanning electron microscope (SEM) observations, that optically massive opal-CT consists of spherical aggregates of blade-shaped crystals (so-called lepispheres; Wise & Kelts 1972, Weaver & Wise 1972, Flörke *et al.* 1976). Flörke *et al.* (1991) showed, by transmission electron microscopy (TEM), that opal-CTLS (optically length-slow) and opal-CTLF (optically length-fast) are composed of aggregates of fibrous and platy microcrystals, respectively.

It was difficult to determine the fundamental structure of opal-CT from X-ray- and electron-diffraction patterns because of diffuse reflections, characterized by very low intensity. Flörke (1955) and Jones & Segnit (1971, 1975) suggested, on the basis of an X-ray-diffraction (XRD) analysis, that the fundamental structure of opal-CT is that of cristobalite, whereas Mitchell & Tufts (1973) and Wilson

[1] *E-mail address*: nagase@mail.cc.tohoku.ac.jp

et al. (1974) proposed instead the structure of tridymite, on the basis of X-ray- and electron- diffraction patterns. Recently, many detailed analyses of the structure of opal-CT were carried out using several methods: high-resolution TEM (Rice & Elzea 1993, Cady & Wenk 1994, Rice *et al.* 1995, Elzea & Rice 1996, Cady *et al.* 1996), XRD (Graetsch *et al.* 1987, 1994, Flörke *et al.* 1990), XRD pattern simulation (Graetsch & Flörke 1991, Graetsch *et al.* 1994, Guthrie *et al.* 1995) and ^{29}Si nuclear magnetic resonance (NMR) methods (de Jong *et al.* 1987, Graetsch *et al.* 1994). Most results of these studies agree well with the model proposed by Flörke (1955), in which opal-CT is composed of interstratified cristobalite and tridymite. Among these studies, the high-resolution TEM (HRTEM) analyses of Elzea & Rice (1996) and Cady *et al.* (1996) provide direct images of the stacking sequence in opal-CT crystals.

Opal-CT is recognized as a precursor of quartz at the transformation stage from biogenic amorphous silica (opal-A) to quartz during the diagenesis of siliceous sediments (*e.g.*, Hesse 1988). The XRD pattern of opal-CT gradually changes to that of opal-C, composed of more ordered cristobalite crystals compared to opal-CT, with a decrease in the spacing of the strongest reflection at ~21.7° (CuKα) as a result of the recrystallization (Murata & Nakata 1974). The spacing of the strongest reflection corresponds to d_{101} of low cristobalite and d_{001} of low tridymite [we refer the structure of tridymite to the pseudo-orthorhombic structure refined by Konnert & Appleman (1978)], and the d value of the strongest reflection is typically reported as "d_{101}". The volume ratio of interstratified cristobalite and tridymite in the crystal is known to be a function of the d_{101} value. A comparison of calculated XRD patterns with those measured from samples indicated that opal-CT and opal-C contain 30–50% and 20–30% tridymite-type stacking, respectively (Graetsch *et al.* 1994). However, Guthrie *et al.* (1995) showed that the XRD patterns of opal-CT are influenced not only by the proportion of cristobalite and tridymite, but also by several other factors, such as particle size and degree of order of the stackings. Elzea & Rice (1996) analyzed the XRD patterns of opal-CT in detail and integrated their findings with TEM

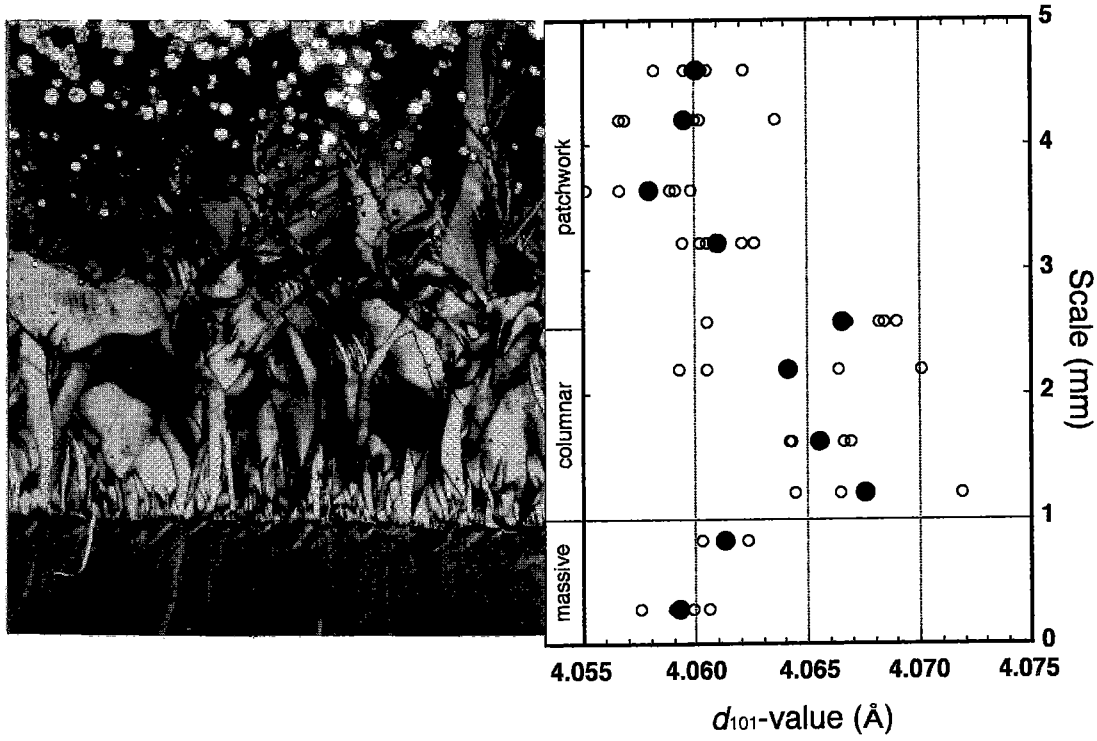

FIG. 1. Cross-polarized optical photomicrograph of columnar texture of opal-CT from the Hosaka opal mine and corresponding d_{101} values. The thin section was cut normal to the horizontal layer of a silica- rich geode. Spherulites of chalcedony are included in the upper parts (white blotches). The d_{101} values were measured using a Guinier–Hägg camera. The solid circles represent the average of the measured values shown by the open circles.

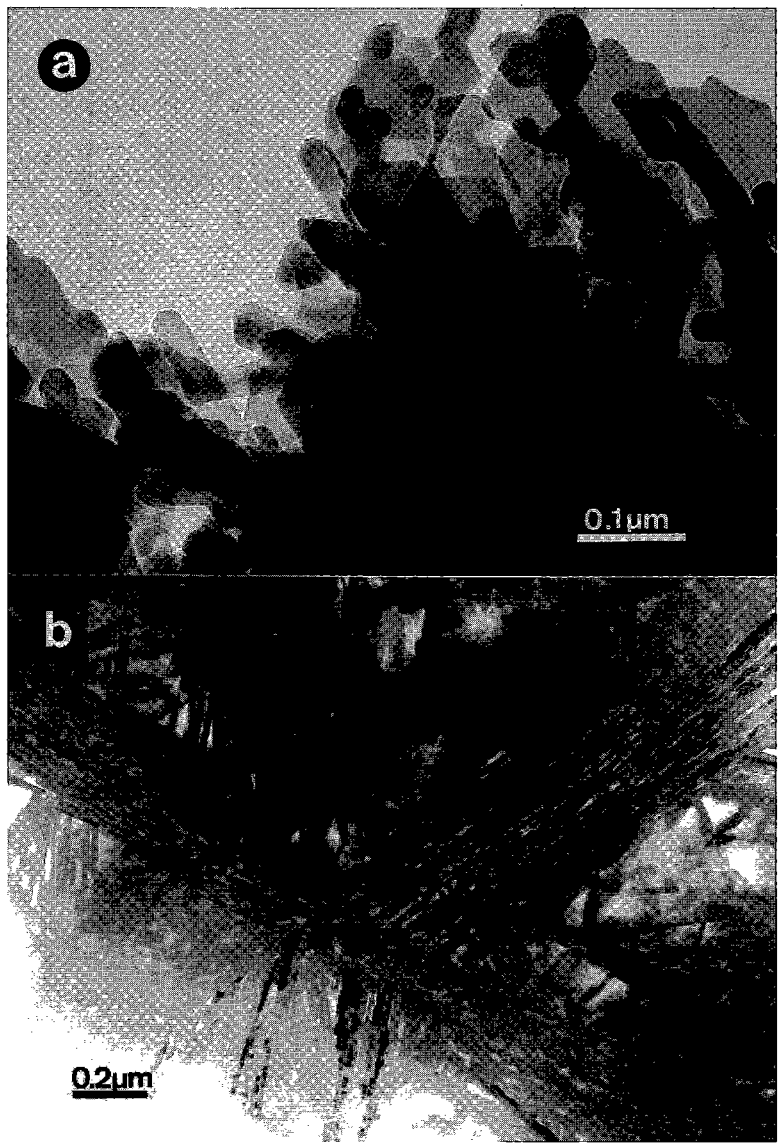

FIG. 2. TEM images of opal-CT lepisphere from the Hosaka opal mine. The same sample was prepared by (a) dispersion on a microgrid and (b) an ion-thinning method. The criss-cross blades of the lepisphere are composed of aggregates of polygonal and platy crystals, and the cross section of the lepisphere shows a fibrous texture.

observations. They showed that the degree of the stacking disorder reaches a maximum at the d_{101} value of about 4.09 Å. They also suggested that tridymite domains are common in samples of opal-CT with d_{101} values larger than 4.09 Å. Cady *et al.* (1996) carried out detailed HRTEM observations for the structure and texture of opal-CT from sedimentary rocks, and concluded that burial diagenesis is responsible for the epitactic growth of ordered cristobalite on disordered opal-CT crystal and for a solid-state transformation from opal-CT to quartz.

Most opal-CT in volcanic rocks is considered to precipitate directly from supersaturated solutions; thus

the transformation of opal may not occur in the volcanic environment (Flörke *et al.* 1990) The volcanic-type opal-CT and opal-C show some differences and yet some similar textural and structural characteristics compared to those in sedimentary rocks. Thus, the objectives of our study are to describe the internal texture and crystal structure of opal-CT and opal-C from silica nodules in volcanic rocks using TEM, SEM and optical microscope observations, and to elucidate the growth process of volcanic-type opal-CT and opal-C.

Samples

The opal specimens used for this study were collected from the Hosaka opal mine, Fukushima Prefecture, Japan (Tsutsumi & Sakamoto 1973) and the Akase opal mine, Ishikawa Prefecture, Japan. Many spherulites of fibrous anorthoclase, up to ten centimeters in diameter, occur in rhyolite and perlite from these opal mines. The spherulites are considered to be produced by devitrification of rhyolite glass (Akizuki 1983). The spherulites of anorthoclase include a lens-like silica-rich geode at the core. The silica-rich geode consists of opal and chalcedony, with some originally horizontal layers from one to several millimeters in thickness.

On the basis of X-ray powder-diffraction analyses, the samples were grouped into chalcedony and three types of opal: opal-A (amorphous pattern), opal-CT ($d_{101} > 4.07$ Å) and opal-C ($d_{101} < 4.07$ Å). The chalcedony is colorless and transparent to translucent, whereas opal samples are commonly whitish to pale bluish in color, and opaque without opalescence. Opal showing opalescence is rare in the samples examined, and is composed of opal-A. Most of the opal samples consist of opal-CT and opal-C, and the d_{101} value varies from 4.05 to 4.09 Å. Two types of texture can be recognized in opal-CT using optical microscopy: isotropically massive (opal-CT_M) and columnar (Fig. 1). Lepispheres of opal-CT are common in samples of opal from sedimentary rocks, although samples showing a lepispheric texture under the SEM are rare among those examined. Textures of opal-CT lepispheres were observed to consist of opal-CT_M and columnar opal-CT. The following three representative samples were examined in detail: (1) opal-CT lepispheres from the Hosaka mine; aggregates of fine-grained lepispheres occur rarely in a layer between chalcedony layers from this mine; (2) opal-CT showing columnar texture from the Hosaka mine; the texture of this sample is most common in the opal-CT samples from the two mines; (3) opal-C from the Akase mine; the X-ray powder-diffraction pattern of this sample is that of highly ordered low cristobalite with a very weak shoulder at 4.3 Å.

Experimental Methods

The samples were cut in the orientation normal or parallel to the horizontal layer of the silica-rich geode, and thin sections were made for observation with an optical microscope (polarized light). The cut faces were polished and then etched with a concentrated HF solution (48 wt.%). The etched cross-sections were observed using an SEM (JEOL JSM T–330A) after deposition of a gold coating. Thin foils for TEM observations were supplied from petrographic thin sections, and were prepared by an Ar ion-thinning method, with cooling using liquid nitrogen. The sample of opal-CT lepispheres was also dispersed in acetone and pipetted onto holey carbon TEM microgrids. TEM observations were carried out using a JEOL JEM–2010 type transmission electron microscope operated at an accelerating voltage of 200 kV. Electron-diffraction patterns were obtained using a selected-area aperture by which the area giving the diffraction pattern is limited to 400 nm in diameter. After the photographs of the diffraction pattern were taken using a low-dose electron beam, corresponding TEM images were obtained. HRTEM images were interpreted to provide information of the structure of opal-CT by comparison with simulated images calculated using the MacHREM multislice program (Ishizuka 1980, Ishizuka & Ueda 1977). Various types of structure have been reported for natural and synthetic low tridymite (*e.g.*, Dollase & Baur 1976, Kato & Nukui 1976, Nukui & Nakazawa 1980, Hoffmann *et al.* 1983); the crystallographic data of the pseudo-orthorhombic (PO-type) structure analyzed by Konnert & Appleman (1978) was used for the image simulation of the tridymite. Image simulation in the case of cristobalite was carried out using the data reported by Schmahl *et al.* (1992). The d_{101} values were measured using a Guinier–Hägg camera with Cu$K\alpha$ radiation (Kitakaze 1992).

Results

Texture of opal-CT lepispheres from the Hosaka opal mine

Opal-CT lepispheres from the Hosaka opal mine are composed of aggregates of criss-crossing blades, which are several micrometers in diameter, as seen under the SEM. A TEM image of a dispersed sample on a microgrid shows a polygonal and platy morphology of the crystals (Fig. 2a), with prominent (101) faces showing a pseudo-hexagonal diffraction pattern of pseudomerohedral twinning on the [010]*–[$\bar{1}$02]* net of low cristobalite. The thin crystal is much smaller in size than the blade observed under the SEM. The cross section of the lepisphere shows a fibrous texture (Fig. 2b). The blade corresponding to that in the SEM image is composed of aggregates of such thin crystals, which are roughly parallel in orientation to each other in the blade. The thin crystal is several tens of nanometers in thickness and less than 0.5 μm in length and width, which agrees with the platy crystal observed in the dispersed sample. The angle between [101]* directions of two crossed blades is about 70°, which correlates with the angle between two {101} planes of low cristobalite. The cross-section of the lepisphere is similar in texture to that of opal-CT crystals from sedimentary rocks, as studied by Cady *et al.* (1996).

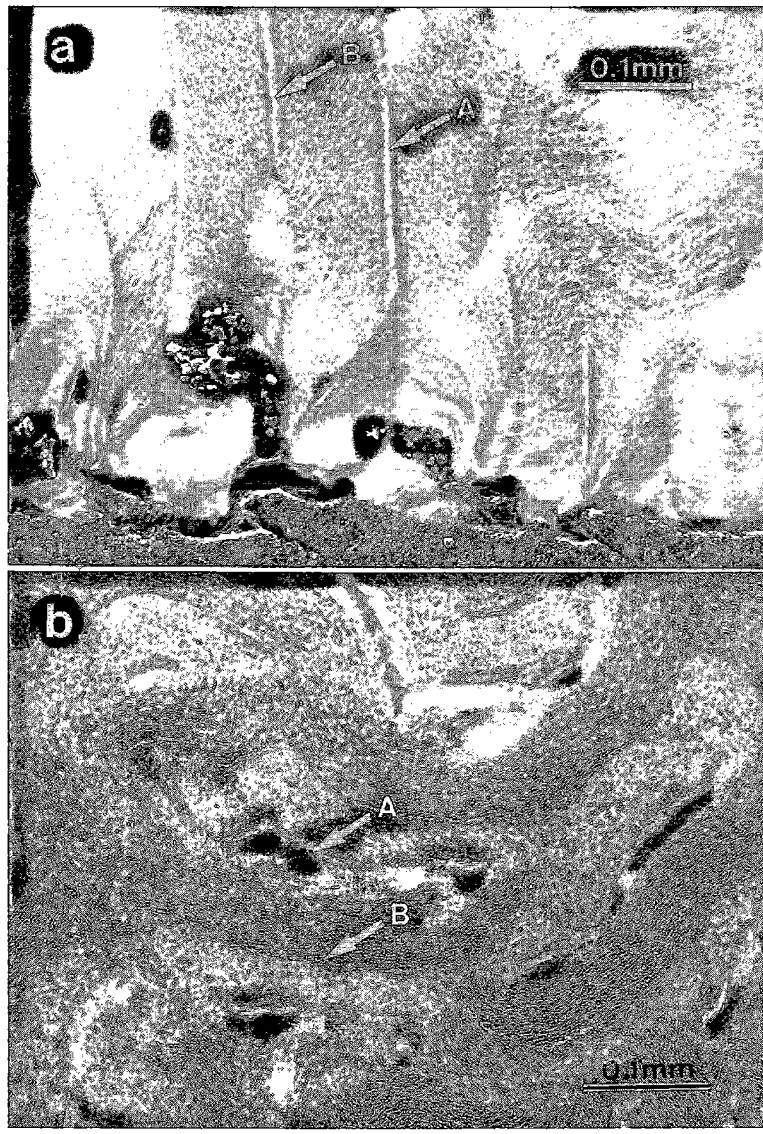

FIG. 3. SEM photomicrographs of columnar texture of opal-CT cut (a) parallel and (b) normal to the horizontal layer of a silica-rich geode. Photographs were taken on the etched surface after polishing. The column cut normal to the layer is irregularly circular to oblong, with fine striations. Vermicular pattern (arrow A) and boundary (arrow B) in (b) correspond to the boundaries shown by arrows A and B in (a), respectively.

Columnar texture of opal-CT

Figure 1 shows an optical microphotograph of a layer of opal-CT showing the typically columnar texture. The thin section is normal to the horizontal layer of the silica-rich geode. Figure 3a shows an etched pattern of the columnar texture, in which fine striations are inclined at about 20–40° with respect to the elongation of the column. The direction of optical extinction is parallel to the striation. The directions of striations in two adjacent columns are inclined in opposite sides to each other, so that the paired columns show a relationship like in the case of a twin seen in thin section under the optical microscope. Figure 3b shows an etched pattern of the section cut parallel to the horizontal layer of the silica-rich geode. The cross section shows an irregularly circular texture with fine

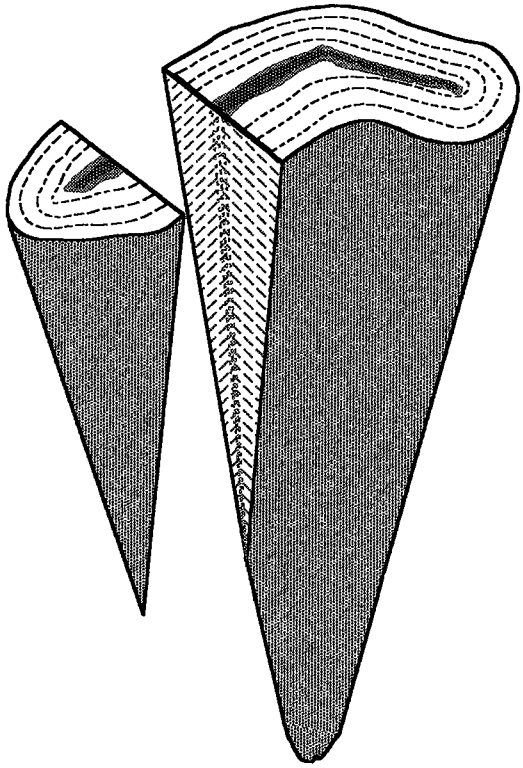

FIG. 4. Schematic illustration of three-dimensional conical form of a pair of columns.

striations. A vermicular pattern shown by arrow A in Figure 3b corresponds to boundaries of the columns, shown by arrow A in Figure 3a. Also, the boundary (shown by arrow B in Fig. 3b) of the irregularly circular feature corresponds to a distinct or indistinct boundary (shown by arrow B in Fig. 3a). The paired columns as shown in Figure 3a correspond to one circular-feature domain in Figure 3b, such that it is not a twin. From these observations, we suggest that the three-dimensional form of the paired columns is conical, as illustrated in Figure 4.

Figure 5a shows a TEM photomicrograph of the internal texture of the column in a section cut normal to the horizontal layer of the silica-rich geode. The column exhibits a fibrous texture composed of thin crystals, whose thickness is several tens of nanometers and whose length is less than 1 m. The fibers correspond to the striations shown in the SEM image (Fig. 3a) and are roughly parallel to each other. Along the boundary of the columns, the directions of the fibers seem randomly oriented. From optical and TEM observations, the fiber is optically length-slow. The fiber axis is parallel to (101) of low cristobalite and (001) of low tridymite. The structure of the opal-CT crystal is described in detail in the following section. A similar fibrous texture is observed in a section cut parallel to the horizontal layer of the silica-rich geode.

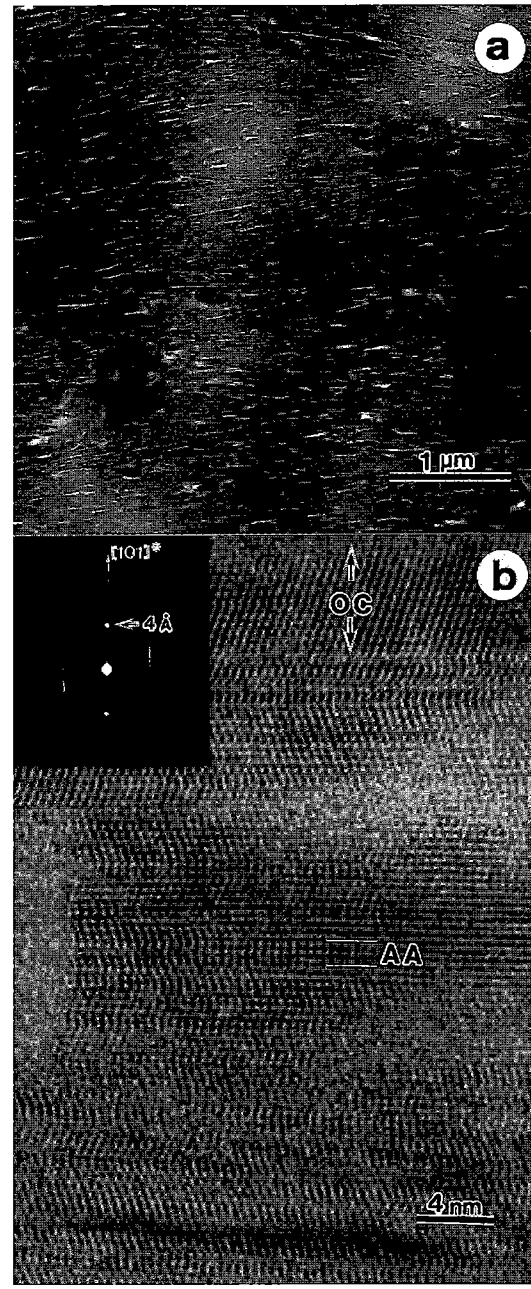

FIG. 5. TEM images of opal-CT crystals in the columnar texture. a) Fibrous texture, which is inclined to the thin and platy crystals. b) Lattice image and corresponding electron-diffraction pattern of the opal-CT crystal. The horizontal direction of the photograph (b) is parallel to the crystal elongation in (a). The a^*–c^* plane of low cristobalite is parallel to the photograph, and the orientation of the sheets of SiO_4 tetrahedra is horizontal. The stacking sequence indicated by AA in (b) contains antiphase domain boundaries. OC: ordered cristobalite.

Although the crystals seem fibrous (Fig. 5a), the crystals that give an [010]*–[$\bar{1}$02]* diffraction pattern of low cristobalite are not fibrous, but rather polygonal and platy. Therefore, we suggest that the crystals in the column are very thin and platy, as shown in Figure 2a. The section inclined to the plates shows a fibrous texture because of the parallel growth of extremely thin crystals.

The opal-CT_M layer (optically massive layer in Fig. 1), below the layer showing the columnar texture, is composed of intersecting aggregates of blades, according to TEM observations. The cross-section of intersecting aggregates in the opal-CT_M layer is similar in texture to that of the lepisphere shown in Figure 2b, and the blade also consists of a parallel growth of the thin platy crystals. However, in the case of the opal-CT_M, the interstitial space among the spherical aggregates is filled by ordered cristobalite crystals; this feature will be described in detail in the following section. The platy crystals gradually change from a random orientation in the massive-textured domain to a roughly parallel orientation in the domains having a columnar texture.

The columns showing a strong birefringence gradually become slender during growth, and more weakly birefringent parts, which are homogeneously etched, develop among the slender columns. This texture was described as a "patchwork pattern" by Flörke *et al.* (1991). Our TEM observations reveal that the part showing a weak birefringence consists of platy crystals as well. The thin crystals are in roughly parallel orientation to each other in the blade (or bundle). From measurements with the TEM, the size of the thin crystals slightly decreases with the change in texture, from the columnar to the patchwork pattern. The blade is less than 0.2 μm in thickness and 1–3 μm in length. The orientation of the blades is more irregular in the weakly birefringent part than in the strongly birefringent part; in fact, the blades cross each other.

Structure of opal-CT from the Hosaka opal mine

Figure 5b shows a HRTEM image and corresponding electron-diffraction pattern of a crystal in the columnar texture of opal-CT from the Hosaka opal mine. The horizontal direction of the photograph is parallel to the crystal's elongation shown in Figure 5a. The spacing of the horizontal fringe in the lattice image is about 4 Å, which agrees with d_{101} of low cristobalite. The vertical direction is normal to the sheets of SiO_4 tetrahedra, and the image corresponds to the (010) projection of low cristobalite and the (100) projection of low tridymite. The diffraction pattern is heavily streaked along the <101>* direction of the low cristobalite sequence, and the streakings imply that the crystal includes numerous planar faults parallel to (101) of low cristobalite. HRTEM images on a corresponding projection were simulated for low cristobalite and low tridymite (Fig. 6). As shown in the simulated images, these stacking sequences are denoted

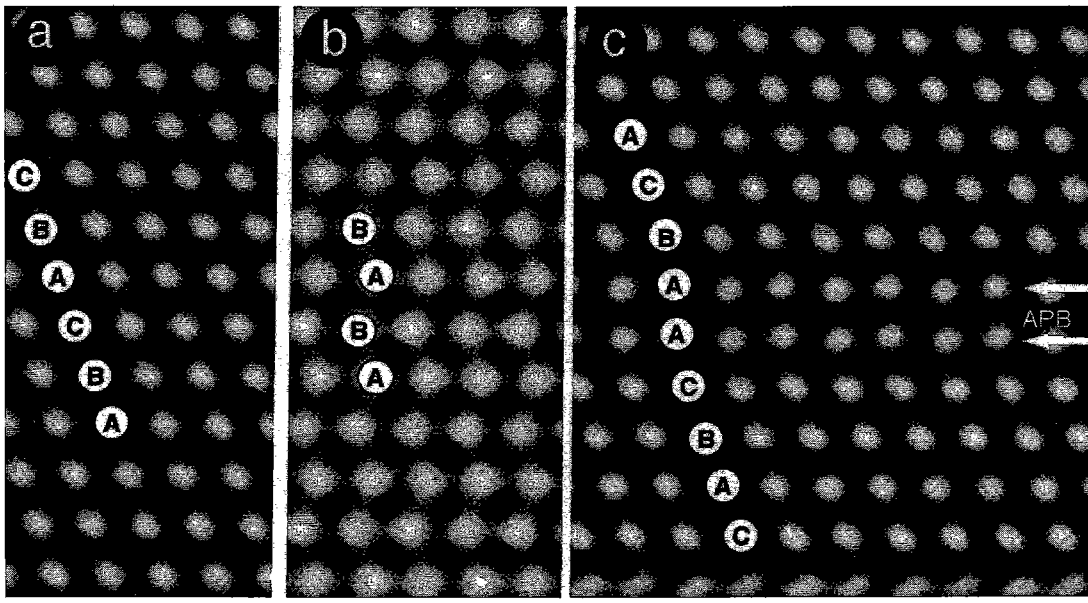

FIG. 6. Simulated images of (a) low cristobalite, (b) low tridymite and (c) antiphase domain boundary in low cristobalite. The images are projected on the (010) of low cristobalite and the (100) of low tridymite, and the vertical is the stacking direction of the sheets. The arrows in (c) show antiphase twin boundaries (APB).

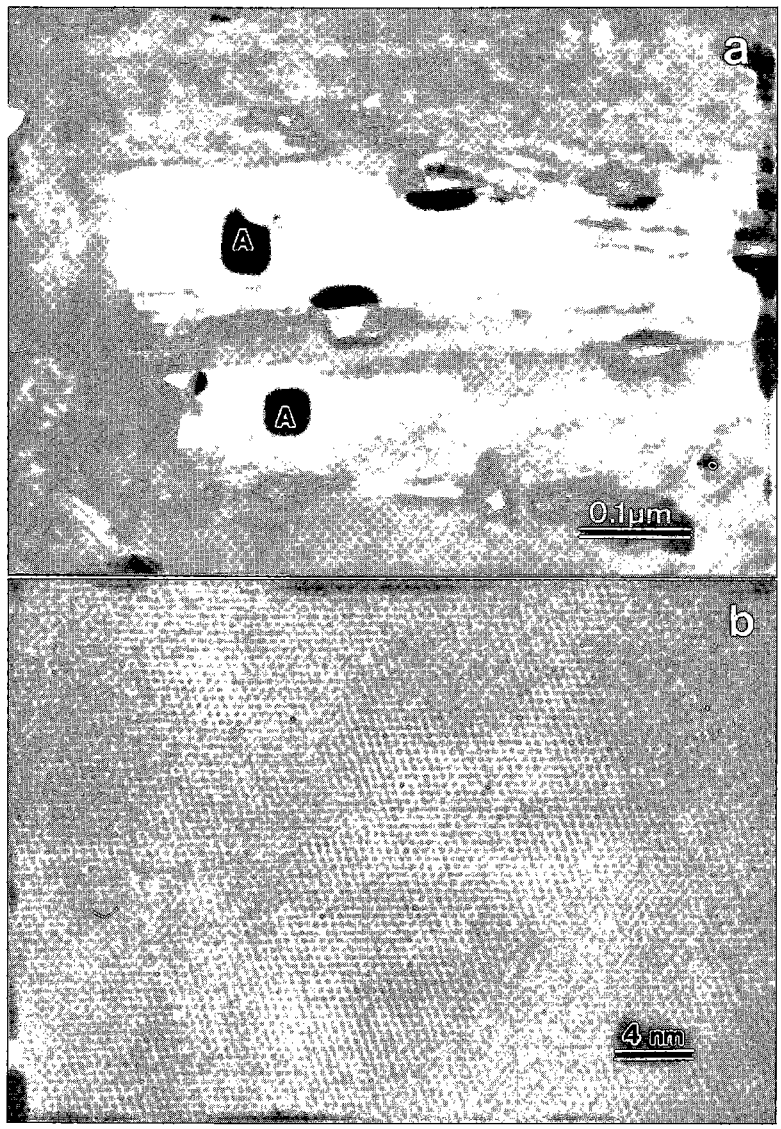

FIG. 7. TEM images of opal-CT crystals in the patchwork pattern texture. The dark areas, shown by A in (a), consist of well-ordered stackings of cristobalite as shown in (b). The orientation in (a) is the same as in Figures 5 and 6.

by triple (*ABC*) and double (*AB*) periodicities, respectively. A careful comparison of the simulated images with the HRTEM images of opal-CT shows that most of the stacking sequences agree with that of cristobalite, although the crystal includes numerous stacking faults. The {101} twin fault of cristobalite (..*CBABC*..) includes a stacking sequence of tridymite (*BAB*), but the successive stacking sequence of tridymite is less than three layers thick in the lattice image. Elzea & Rice (1996) observed domains of ordered tridymite in opal-CT samples with a HRTEM and showed a lattice image for a domain of tridymite having a thickness of about 4 nm (10 layers). However, such successive stackings of tridymite were not found out in our samples. Careful observations of the lattice images show that the stacking sequence of tridymite occupies about 20% in the area, and that most of the stackings of tridymite are located at the twin faults of the cristobalite. Whereas the inner area of the crystal is composed of disordered stackings, the periphery (OC in Fig. 5b) has ordered stackings of cristobalite. The crystallographic orientations of the domains

of ordered and disordered cristobalite are parallel with each other in the crystal, and the boundary between the these domains is coherent.

AA sequences are locally observed in the lattice image and in some cases repeat in a few sequences (arrows AP in Fig. 5b). Nord (1992) and Heany (1994) suggested that low cristobalite includes three types of transitional twins: antiphase domain, pseudomerohedral and enantiomorphic twins. Among these possibilities, the AA sequence in Figure 5b most agrees with a simulated image of a stacking sequence at antiphase domain boundaries (Fig. 6c). The antiphase domains are related by the lost translation vector 1/2[111] in low cristobalite, and the simulated image was calculated for the case of two successive boundaries parallel to the (101) plane. In Figure 5b, the antiphase domain boundaries continue for several nanometers in the direction parallel to the sheet of SiO_4 tetrahedra, and they gradually change to the stacking sequence of cristobalite or tridymite.

The orientation of the sheets of SiO_4 tetrahedra in the lattice image is not always exactly parallel. The presence of slight misfits of the stacking causes a mosaic structure with slight differences in crystallographic direction. Thus, the strong streaking on the electron-diffraction pattern is caused by the disorder in the stacking sequence. Furthermore, the diffraction pattern rotates slightly because of the mosaic structure.

Figure 1 shows a relationship between variation of d_{101} values and corresponding optical texture of opal-CT from the Hosaka opal mine. A distinct relationship can be seen between the d_{101} values and texture: the d_{101} values are relatively large in domains showing columns, and are smaller in parts that are massive or that show a patchwork pattern. TEM observations commonly show evidence that the crystals in the patchwork pattern consists of domains of highly ordered cristobalite with area of disordered cristobalite (Fig. 7). The ordered cristobalite develops epitactically at the end of platy crystals, and, therefore, seems to surround the disordered cristobalite. With decreasing d_{101} value, the area occupied by the ordered domains increases in the crystal; however, the disordered domains do not show a diagnositc difference in degree of order in the stacking sequence and in the proportion of the stacking sequence of tridymite.

Opal-C from the Akase opal mine

Grayish blue opal-C from the Akase opal mine was studied with the same approach. As described above, the

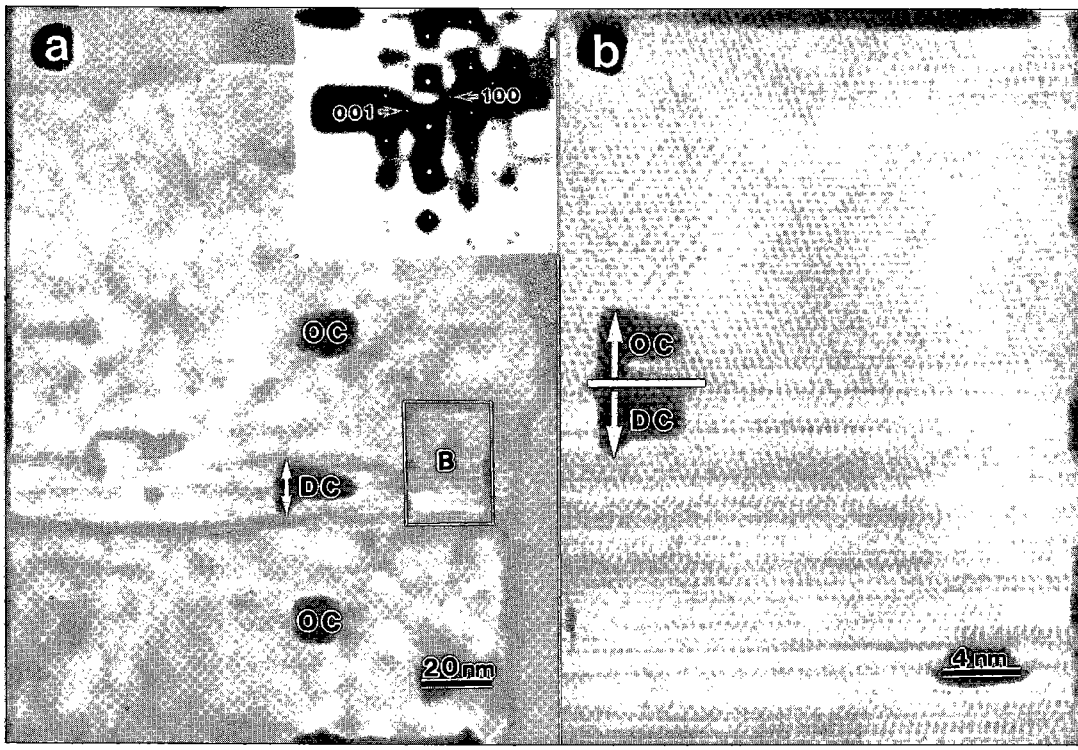

FIG. 8. Lattice image and electron-diffraction pattern of opal-C crystal from the Akase opal mine. The opal-C crystal shows a texture indicative of epitactic growth of well-ordered cristobalite (OC) on a domain of disordered cristobalite, indicated by DC in (a). High-magnification photomicrograph (b) corresponds to rectangle area B shown in (a). The orientation is the same as in Figure 6.

X-ray powder-diffraction pattern for the sample shows highly ordered low cristobalite, with a weak shoulder peak at 4.3 Å. The crystals are octahedral in form and ~0.1–0.5 m in diameter under the SEM. Figure 8 shows TEM images and the corresponding electron-diffraction pattern of the opal-C crystal, and the pattern is that of the a^*–c^* net of low cristobalite. The crystal indicates the {101} twinning in the diffraction patterns, but the patterns have sharper reflections and weaker streaks than those of opal-CT. A small area of disordered cristobalite is present at the center of the crystal, as also shown in Figure 5b, whereas most of the crystal has the structure of highly ordered cristobalite, with few stacking faults. The domains of disordered and ordered cristobalite show a large difference in degree of order in the stacking sequence, and it is possible to distinguish disordered cristobalite from ordered cristobalite. The crystallographic orientations are parallel with each other, *i.e.*, common in both disordered and ordered cristobalite domains. The boundary between disordered and ordered cristobalite is coherent and relatively distinct (Fig. 8b).

Discussion and Conclusions

On the basis of observations by optical microscopy, the textures of opal-CT samples from the two mines were classified as one of two types, columnar and massive (opal-CT_M). The TEM observations suggest that both of the textures really consist of thin platy crystals, although the thin platy crystals look fibrous in cross section.

During the course of this study, we found that the columnar texture is a common feature in most volcanic-type opal-CT. Although each column appears to be a single crystal under the optical microscope, it really consists of a roughly parallel growth of platy microcrystals, as revealed by the TEM observations.

Opal-CT_M is composed of criss-crossing aggregates of blades, and, therefore, the birefringence of the opal-CT_M is weak. Each blade is composed of a roughly parallel growth of thin platy crystals. The TEM image of opal-CT_M is similar in texture that of the lepispheres, with a difference in size of the thin crystals. Under the SEM, most of the samples of opal-CT_M show homogeneously etched patterns, without a distinct texture such as lepispheres. The reason for the difference in the SEM images is that ordered cristobalite infills interstices between the blades in opal-CT, whereas the interstices are not infilled in the lepisphere-bearing samples. The disordered opal-CT, consisting of the blades of lepispheres, is more rapidly etched than ordered cristobalite, so that the SEM image of etched opal-CT_M shows a pattern of residual ordered cristobalite after the lepispheres are dissolved. A few samples of opal-CT_M in which opal-A infills the interstices among the spherical aggregates show a lepispheric pattern of etching under the SEM.

The HRTEM observations show that opal-CT from the two opal mines contains few repeats of the tridymite stacking sequence compared to samples observed by Elzea & Rice (1996). Opal-CT was not found without ordered cristobalite domains in our samples, and all the opal-CT crystals contain domains of ordered cristobalite, although these ordered domains are limited to the thin periphery of the crystal in some samples (Fig. 5b). Volcanic-type opal-CT seems to include more of the ordered cristobalite domains than opal-CT of the sedimentary type. The opal-CT and opal-C samples from the two mines have a relatively small average d_{101} value (4.07 Å) in the X-ray-diffraction analyses, compared to the range of the d_{101} values of sedimentary-type opal-CT and opal-C (4.04–4.12 Å). Opal-CT crystals with small values of d_{101} were synthesized at relatively high temperatures by Mizutani (1966, 1977). The experimental results suggest that volcanic-type opal-CT grew at a higher temperature than sedimentary-type opal-CT. The d_{101} value of the sample with the smallest content of the ordered cristobalite is 4.09 Å. This value corresponds to that of the crystal that shows the greatest disorder of stacking in samples analyzed by Elzea & Rice (1996). We suggest that the stacking of tridymite may be present in opal-CT in which the d_{101} value is greater than 4.09 Å.

The samples of opal-CT and opal-C from the two opal mines are composed of highly ordered and disordered cristobalite domains, respectively. Domains of disordered cristobalite commonly are enclosed by domains of ordered cristobalite, and the domain boundary is coherent, as seen in the TEM images. Where the d_{101} value of the opal-CT determined by X-ray diffractometry is shifted toward a smaller value, domains of highly ordered cristobalite have developed in the crystal. XRD patterns of opal-CT ($4.09 < d_{101} < 4.11$ Å) are not only influenced by the proportion of cristobalite and tridymite sequences in the crystal, but also by the particle size and the degree of order (Guthrie *et al.* 1995). The particle size is expected to increase with decreasing value of d_{101}. However, the Hosaka opal-CT shows the opposite relationship. Furthermore, samples containing disordered cristobalite domains do not show a distinct relationship between degree of stacking disorder and d_{101} value. In the case of the volcanic-type opal-CT, the d_{101} value is strongly correlated with the volume ratio of ordered and disordered cristobalite domains in the crystal.

Well-ordered, non-opaline cristobalite commonly has an octahedral habit, with prominent {101} faces (Frondel 1962). Even though opal-CT has the structure of cristobalite, all the opal-CT crystals exhibit a platy morphology. In our samples, only the Akase opal-C shows a distinctly octahedral habit. We suggest that the presence of planar defects is correlated with the platy morphology. The structure has many stacking faults parallel to the sheets of SiO_4 tetrahedra, whereas the structure is ordered in the plane of the sheets. In the HRTEM images of the opal-CT, the interstratifications of cristobalite and tridymite have no periodicity, such as in a highly ordered polytype. Smith & Yoder (1956) suggested that randomly stacked structures occur when crystal growth proceeds by secondary nucleation, and that the degree of order is controlled by

bond strength in the structure. Growth by secondary nucleation occurs in more highly supersaturated solutions than spiral growth. The opal-CT grew from thin and platy nuclei, and the platy habit was enhanced by the secondary nucleation growth process, leading to the development of stacking faults in the structure. As a result, highly disordered cristobalite shows a platy form. With decreasing degree of supersaturation in the solutions, as a result of the precipitation of the crystals, the growth mechanism changes from secondary nucleation to spiral growth. If the crystal had grown by the spiral-growth mechanism, a more ordered structure of cristobalite would be expected. Furthermore, in the case of more slowly grown crystals, the habit is expected to change from platy to octahedral, and the stackings become highly ordered. In the opal-C from the Akase mine, domains of disordered cristobalite at the center of the crystal are overgrown by highly ordered cristobalite. These textures reveal a change in the growth process.

Acknowledgements

We are grateful to Drs. S. Kojima and T. Kakegawa for valuable suggestions on this manuscript. Thanks are also due to Dr. A. Kitakaze for useful discussion concerning the X-ray-diffraction method, and to Messrs. E. Aoyagi and T. Ohyama for their kind advice on preparation of the TEM samples. We thank Prof. R.F. Martin and anonymous referees for helpful reviews of an earlier version of the manuscript. This study was partially funded by Grant-in-Aid for Scientific Research (No. 05740330) from the Ministry of Education, Science and Culture of Japan.

References

Akizuki, M. (1983): An electron microscopic study of anorthoclase spherulite. *Lithos* **16**, 249-254.

Cady, S.L. & Wenk, H.-R. (1994): Diagenetic microcrystalline opal varieties from the Monterey Formation, CA: HRTEM study of structures and phase transition mechanisms. *Geol. Soc. Am., Abstr. Programs* **26**, A112.

_____, _____ & Downing, K.H. (1996): HRTEM of microcrystalline opal in chert and porcelanite from the Monterey Formation, California. *Am. Mineral.* **81**, 1380-1395.

De Jong, B.H.W.S., Hoek, J.V., Veeman, W.S. & Manson, D.V. (1987): X-ray diffraction and ^{29}Si magic-angle-spinning NMR of opals: incoherent long- and short-range order in opal-CT. *Am. Mineral.* **72**, 1195-1203.

Dollase, W.A. & Baur, W.H. (1976): The superstructure of meteoritic low tridymite solved by computer simulation. *Am. Mineral.* **61**, 971-978.

Elzea, J.M. & Rice, S.B. (1996): TEM and X-ray diffraction evidence for cristobalite and tridymite stacking sequences in opal. *Clays Clay Minerals* **44**, 492-500.

Flörke, O.W. (1955): Zur Frage des "Hoch-Cristobalit" in Opalen, Bentoniten und Gläsern. *Neues Jahrb. Mineral., Monatsh.*, 217-224.

_____, Graetsch, H. & Jones, J.B. (1990): Hydrothermal deposition of cristobalite. *Neues Jahrb. Mineral., Monatsh.*, 81-95.

_____, _____, Martin, B., Röller, K. & Wirth, R. (1991): Nomenclature of micro- and non-crystalline silica minerals, based on structure and microstructure. *Neues Jahrb. Mineral., Abh.* **163**, 19-42.

_____, Hollmann, R., von Rad, U. & Rösch, H. (1976): Intergrowth and twinning in opal-CT lepispheres. *Contrib. Mineral. Petrol.* **58**, 235-242.

Frondel, C. (1962): *The System of Mineralogy*. III. *Silica Minerals*. Wiley, New York, N.Y.

Graetsch, H. & Flörke, O.W. (1991): X-ray powder diffraction pattern and phase relationships of tridymite modifications. *Z. Kristallogr.* **195**, 31-48.

_____, _____ & Miehe, G. (1987): Structural defects in microcrystalline silica. *Phys. Chem. Minerals* **14**, 249-257.

_____, Gies, H. & Topalovic, I. (1994): NMR, XRD, and IR study on microcrystalline opal. *Phys. Chem. Minerals* **21**, 166-175.

Guthrie, G.D., Jr., Bish, D.L. & Reynolds, R.C., Jr. (1995): Modeling the X-ray diffraction pattern of opal-CT. *Am. Mineral.* **80**, 869-872.

Heany, P.J. (1994): Structure and chemistry of the low-pressure silica polymorphs. *Rev. Mineral.* **29**, 1-40.

Hesse, R. (1988): Origin of chert: diagenesis of biogenic siliceous sediments. *Geosci. Can.* **15**, 171- 192.

Hoffmann, W., Kockmeyer, M., Löns, J. & Vach, C. (1983): The transformation of monoclinic low-tridymite MC to a phase with an incommensurate superstructure. *Fortschr. Mineral.* **61**, 96-98.

Ishizuka, K. (1980): Contrast transfer of crystal image in TEM. *Ultramicroscopy* **5**, 55-65.

_____ & Ueda, N. (1977): A new theoretical and practical approach to the multislice method. *Acta Crystallogr.* **A33**, 740-749.

Jones, J.B. & Segnit, E.R. (1971): The nature of opal. I. Nomenclature and constituent phases. *J. Geol. Soc. Aust.* **18**, 57-68.

_____ & _____ (1975): Nomenclature and the structure of natural disordered (opaline) silica. *Contrib. Mineral. Petrol.* **51**, 231-234.

Kato, K. & Nukui, A. (1976): Die Kristallstruktur des monoklinen Tief-Tridymits. *Acta Crystallogr.* **B32**, 2486-2491.

KITAKAZE, A. (1992): Study on the Guinier film reading and calculation methods. *Sci. Rep., Econ. Geol. Res. Project, Univ. Concepcion* **2**, 57-82.

KONNERT, J.H. & APPLEMAN, D.E. (1978): The crystal structure of low tridymite. *Acta Crystallogr.* **B34**, 391-403.

MITCHELL, R.S. & TUFTS, S. (1973): Wood opal – a tridymite-like mineral. *Am. Mineral.* **58**, 717- 720.

MIZUTANI, S. (1966): Transformation of silica under hydrothermal conditions. *J. Earth Sci., Nagoya Univ.* **14**, 56-88.

_____ (1977): Progressive ordering of cristobalitic silica in the early stage of diagenesis. *Contrib. Mineral. Petrol.* **61**, 129-140.

MURATA, K.J. & NAKATA, J.K. (1974): Cristobalitic stage in the diagenesis of diatomaceous shale. *Science* **184**, 567-568.

NORD, G.L., JR. (1992): Imaging transformation-induced microstructures. *Rev. Mineral.* **27**, 455-508.

NUKUI, A. & NAKAZAWA, H. (1980): Polymorphism in tridymite. *J. Mining Soc. Japan, Spec. Vol.* **2**, 364-386 (in Japanese).

RICE, S.B. & ELZEA, J.M. (1993): Stacking disorder in the crystalline opal. *Clay Minerals Soc., Annual Meeting, Abstr. Program*, 137.

_____, FREUND, H., HAUANG, W.-L., CLOUSE, J.A. & ISAACS, C.M. (1995): Application of Fourier transform infrared spectroscopy to silica diagenesis: the opal-A to opal-CT transformation. *J. Sed. Res.* **A65**, 639-647.

SCHMAHL, W.W., SWAINSON, I.P., DOVE, M.T. & GRAEME-BARBER, A. (1992): Landau free energy and order parameter behaviour of the α/β phase transition in cristobalite. *Z. Kristallogr.* **201**, 125-145.

SEGNIT, E.R., ANDERSON, C.A. & JONES, J.B. (1970): A scanning microscope study of the morphology of opal. *Search* **1**, 349-351.

SMITH, J.V. & YODER, H.S., JR. (1956): Experimental and theoretical studies of the mica polymorphs. *Mineral. Mag.* **31**, 209-235.

TSUTSUMI, S. & SAKAMOTO, T. (1973): Opal from Hosaka, Fukushima Prefecture, Japan. *J. Jap. Assoc. Mineral. Petrol. Econ. Geol.* **68**, 295-302 (in Japanese).

WEAVER, F.M. & WISE, S.W., JR. (1972): Ultramorphology of deep sea cristobalitic chert. *Nature* **237**, 56-57.

WILSON, M.J., RUSSELL, J.D. & TAIT, J.M. (1974): A new interpretation of the structure of disordered α-cristobalite. *Contrib. Mineral. Petrol.* **47**, 1-6.

WISE, S.W., JR. & KELTS, K.R. (1972): Inferred diagenetic history of a weakly silicified deep sea chalk. *Trans. Gulf-Coast Assoc. Geol. Soc.* **22**, 177-203.

Received April 27, 1995, revised manuscript accepted July 15, 1997.